Trans Indian Inst Met (2020) 73(7):1743–1753
https://doi.org/10.1007/s12666-020-01988-8

ORIGINAL ARTICLE

Comparative Study on the Cleanliness of Ultra-low Carbon Al-Killed Steel by Different Refining Processes

Shen-yang Song[1] · Jing Li[1] · Wei Yan[1] · Yu-xiang Dai[1] · Yang Liu[1]

Received: 23 January 2020 / Accepted: 30 April 2020 / Published online: 21 May 2020

Abstract Cleanliness of aluminum-killed ultra-low carbon steel produced through BOF–RH–CC and BOF–LF–RH–CC was comparatively investigated by nitrogen–oxygen analysis, SEM analysis and thermodynamic calculation to seek for an optimum refining process. The results show that the non-metallic inclusions with area above 8 μm^2 could be removed obviously in both the refining processes. Compared with BOF–RH–CC process, in RH refining stage, the size of inclusion and total oxygen control were better than the original process. Furthermore, BOF–LF–RH–CC process reduced the inclusion area ratio, the proportion of single inclusion area of < 8 μm^2 increased from 85 to 95%, the proportion of Al_2O_3 inclusion less than 5 μm^2 increased from 50 to 70%. Meanwhile, the desulfurization effect became pronounced and the temperature control of the double refining process was more stable than that of the original process.

Keywords Ultra-low carbon aluminum-killed steel · Deoxidation · Desulfuration · Cleanliness

1 Introduction

Advanced ultra-low carbon Al-killed steel has been widely used in automobiles, household appliances as well as other products because of its high strength, good plasticity and excellent formability [1, 2]. Automobile and household appliances have extremely high requirements for the surface quality of cold-rolled panel. On the contrary, large-sized inclusions in steel are the important cause of surface defects of cold-rolled panel. Therefore, it is important to reduce the amount of inclusions and control inclusion's size during refining process [3–7].

RH refining is a preferred process for mass production of ultra-clean steel because of its advantages in decarburization, deoxidation, inclusions removal, alloying and short processing cycle. So it always associates with BOF and CC to achieve most production of ultra-low carbon Al-killed steel. As is known, Al_2O_3 is the main deoxidation product in Al-killed steel, but it has a terrible impact on the fatigue property of ultra-low carbon Al-killed steel. Liu studied the relationship among the total oxygen content in the steel, the amount of Al inclusion in the steel and steel circulation time during RH refining process. During the first 2 min after aluminum addition, the inclusions in steel are pure Al_2O_3 cluster; 6 min later, the cluster of Al_2O_3 inclusions disappear, the majority of inclusions in steel are globular and massive Al_2O_3 with size of less than 5 μm [7].Moreover, the formation mechanism and morphological evolution of Al_2O_3 inclusion during RH refining process were researched. Some researchers have reported that lower slag oxidizability is beneficial for improving the cleanliness of molten steel during the refining process [8–10].

It is still difficult to achieve stable and satisfying temperature control under low end carbon content for converter steelmaking despite some plants or researchers have applied methods like dynamic converter automatic steelmaking system [11]. In order to ensure continuous casting and regular production of, blowing oxygen, addition of aluminum is usually carried out in the decarbonization stage of RH refining process to heat up, thus increasing the amount of Al and Al_2O_3 inclusion during RH process. More Al_2O_3 inclusion decreases the cleanliness of liquid

✉ Jing Li
lijing@ustb.edu.cn

[1] State Key Laboratory of Advanced Metallurgy, University of Science and Technology Beijing, Beijing 100083, China

steel. At the same time, heating of RH requires oxygen blowing, which will deteriorate the improvement in RH vacuum degree and will be also unfavorable for the improvement in decarburization rate of molten steel [12–14]. In order to ensure the cleanliness of molten steel, long holding time in the ladle after RH vacuum process is always required for ultra-low carbon Al-killed steel usually. A reasonable holding time can improve the cleanliness, but prolonging the holding time long will cause significant temperature drop of molten steel, and further accelerate secondary oxidation of molten steel. Cui studied the influence of the holding time after RH process on the total oxygen content and non-metal inclusion content of IF steel. It is suggested that the holding time should be controlled between 30 and 40 min [15]. Wang established a data mining model to investigate the effect of smelting parameters on the inclusion defect of cold sheet and ranked them as: the total oxygen content before deoxidization in RH > BOF endpoint temperature > temperature before deoxidization in RH. However, Wang et al. didn't propose a better solution to control these parameters [16]. It is therefore necessary to know that how to reduce aluminum addition during RH decarburization process under the condition of stable temperature and improve the cleanliness of molten steel, which are the problems need to solve.

LF refining has functions of heating up, stirring, desulfurization and fine tuning of chemical content. On this basis, introduction of LF furnace into BOF–RH–CC process can not only heat molten steel without aluminum addition but also promote inclusion removal; meanwhile, it provides good conditions to control the sulfur content. This study puts forward a new technological process of BOF–LF–RH–CC, aiming at raising inlet temperature with decreased Al addition and reducing load of inclusion removal during RH process. The refining effects of the two processes were comparatively investigated from the aspects of liquid steel temperature, impurity element content and inclusions evolution.

2 Experimental and Research Methods

2.1 Production Process

In order to compare the difference in control of cleanliness and stability during production of ultra-low carbon Al-killed steel (Table 1) in a domestic steel mill, original

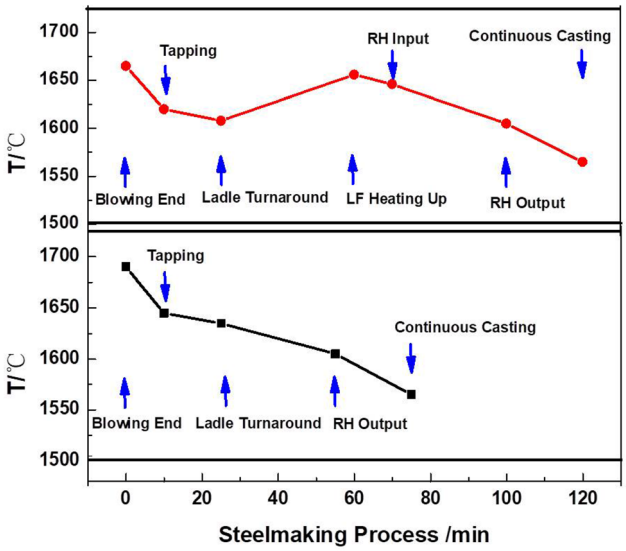

Fig. 1 Ultra-low carbon Al-killed steel time and temperature of steelmaking process

BOF–RH–CC process and new BOF–LF–RH–CC process were conducted. The specific processes are shown in Fig. 1. Generally, BOF–RH–CC process was adopted with a requirement of converter tapping temperature for 1650 °C. Otherwise, oxygen blowing and aluminum particles addition were required to heat molten steel during RH process, and followed by aluminum deoxidation at the end of the decarburization stage, Ti–Fe alloying and a circulation for 6 min. After RH treatment, the molten steel in the ladle remained unstirred for more than 30 min before casting. While for new BOF–LF–RH–CC process, a converter tapping temperature of 1620 °C is enough. Then the molten steel went through argon blowing and heating up for 35 min in LF furnace without slagging, followed by decarburization, aluminum deoxidation, Ti–Fe alloying and a circulation for 6 min in RH furnace. Similarly, the molten steel in the ladle also remained unstirred for more than 30 min before casting.

2.2 Experimental Methodology

Five and four trials were tried to compare the results through original and improved processes, respectively. As shown in Fig. 2, a series of steel samples were taken by bucket sampling device in stage of inlet LF station, leaving LF station, inlet RH station and leaving RH station for each

Table 1 Main chemical compositions of steel (wt%)

C	Si	Mn	P	S	Ti	N	Al_s
< 0.0020	0.005	0.07–0.15	< 0.012	< 0.010	0.060–0.070	< 0.0030	0.028–0.050

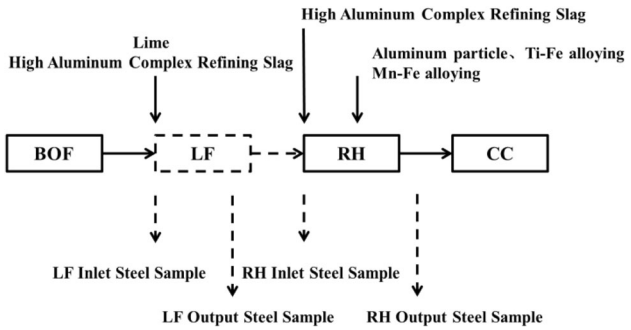

Fig. 2 Secondary refining process sampling

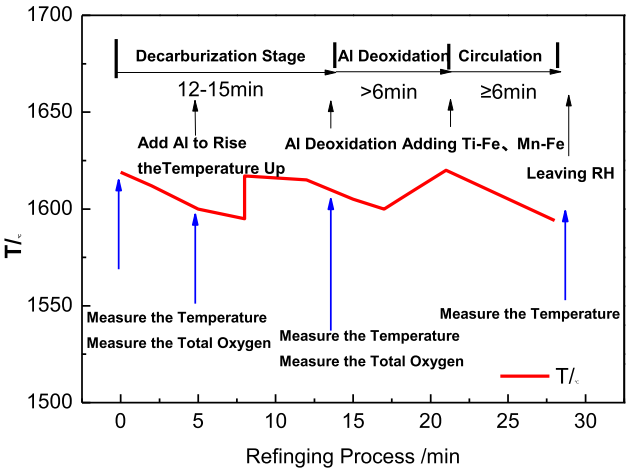

Fig. 3 RH refining operations

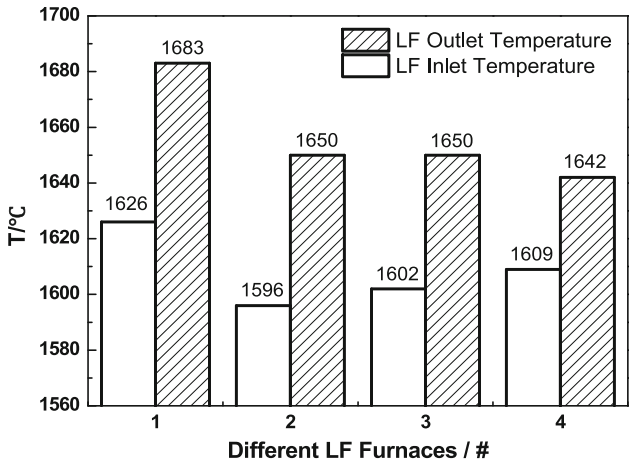

Fig. 4 Temperature variation during in and out of the LF station/°C

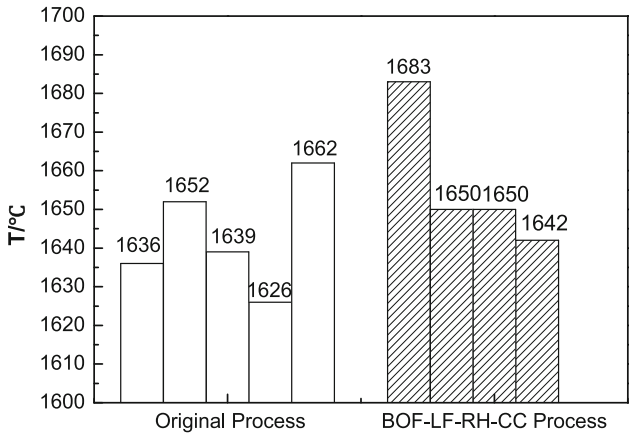

Fig. 5 RH refining inlet temperature/°C

trial; meanwhile, the dissolved oxygen content and temperature in RH process were recorded. RH refining operation is shown in Fig. 3.

Two samples with sizes of Φ5 mm × 7 mm and 15 mm × 15 mm × 10 mm were cut from each bucket steel sample for oxygen and nitrogen content and inclusion analysis, respectively. The cylinder samples were polished with 120 mesh sandpaper until the surface was clean, the total oxygen and nitrogen contents in the samples were measured by an O/N/H analyzer (HORIBA, emga-830, Japan). After being ground and polished using the automatic grinding machine, the square samples were subjected for analysis of morphology, amount, chemical composition of inclusions using inclusion automatic scanning system (ZEISS, EVO18 INCASteel, Germany).

3 Results and Discussion

3.1 Change of RH Inlet Temperature

Figure 4 shows the changes of inlet and leaving temperature of LF furnace in the BOF–LF–RH–CC process. It can be seen that most of inlet temperature is stable at around 1600 °C except the 1st, and then an increase of about 50 °C can be found due to the electrode heating in LF process. Figure 5 shows the RH refining inlet temperature in two different processes. It can be seen that RH inlet temperature is unstable in the original process, which fluctuates between 1626 and 1662 °C, and this can be contributed to the unstable control of converter steelmaking end. On the contrary, RH inlet temperature is more stable in the BOF–LF–RH–CC process, most of them stabilizes at 1650 °C except the 1st. Based on Table 2, the average value of molten steel composition in different processes has been counted out. It can be seen that in the original RH process, average carbon content is 0.028%. According to the converter selective oxidation sequence of Fe–C, it is extremely challenging to control the converter end carbon content of around 0.028%. By adopting the BOF–LF–RH–CC process, the average carbon content at the end point of converter can appropriately increase to 0.041%, which can reduce the difficulty of converter blowing and stabilize the temperature of converter steel.

Table 2 Main chemical compositions of steel during different refining processes (wt%)

	C	Si	Mn	P	S	Ti	T.O.	N	Als
BOF–LF–RH–CC process									
LF inlet	0.041	0.004	0.100	0.012	0.010	–	0.0500	–	0.004
LF outlet	0.044	0.004	0.077	0.008	0.003	–	0.0300	–	0.012
RH inlet	0.044	0.004	0.077	0.008	0.003	–	0.0300	–	0.012
RH outlet	0.0015	0.004	0.125	0.008	0.003	0.066	0.0070	0.002	0.04
Original process									
RH inlet	0.028	0.004	0.080	0.008	0.006	–	0.0450	–	0.005
RH outlet	0.0015	0.004	0.125	0.008	0.006	0.066	0.0080	0.002	0.04

3.2 Change in Aluminum Addition in RH Refining

Due to the instability of RH inlet temperature in the original process, addition of Al particles is needed to increase temperature during RH refining process. The functions of Al addition in the process of RH refining are temperature-rising, deoxidation and alloying. Compared with the original BOF–RH–CC process, the introduction of LF furnace make RH inlet temperature more stable in BOF–LF–RH–CC process, and therefore the function of Al addition in BOF–LF–RH–CC process changes to deoxidation and alloying.

The decarburization time of RH refining process is about 15 min. The temperature after the beginning of decarburization for 5 min determinesa the amount of Al particles should be added into the RH decarburization stage. If the temperature after the beginning of decarburization for 5 min is lower than 1610 °C, Al particles should be added in the furnace to increase molten temperature. The temperature needed to be higher than 1610 °C for 5 min, which is concluded according to the superheat demand of steel continuous casting and field production data. Figure 6 shows the ratio of oxygen blowing during heating up in RH decarburization stage. When decarburization temperature for 5 min is less than 1610 °C, Al addition rate is up to as much as 86.4%, while Al addtion rate is only about 11.1% for the temperature is greater than 1610 °C. As can be seen from the above discussion, stabilizing RH decarburization temperature for 5 min above 1610 °C can reduce the Al addition to improve the heat-up ratio effectively.

In the RH refining decarburization stage, the reaction heating during oxygen blowing and Al particles addition are given by the following formulae.

$$Q_{c_1} = -2.3 \cdot W_{\mathrm{Al}} \cdot \Delta H_1 \tag{1}$$

$$Q_{c_2} = W_{\mathrm{steel}} \cdot [\%\mathrm{O}] \cdot \Delta H_2/32 \tag{2}$$

$$Q_c = Q_{c_1} + Q_{c_2} \tag{3}$$

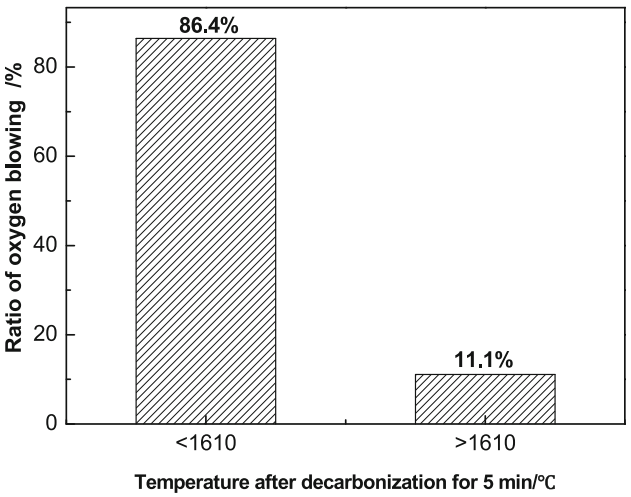

Fig. 6 Ratio of oxygen blowing in RH decarburization stage

$$T_{\mathrm{up}} = \frac{Q_C}{C_{\mathrm{P}} \cdot W_{\mathrm{steel}}} \tag{4}$$

$$\Delta H_1 = -2.3 \times 10^6\,\mathrm{J/kg} \tag{5}$$

$$\Delta H_2 = -22.3 \times 10^6\,\mathrm{J/kg} \tag{6}$$

$$C_{\mathrm{P}} = 0.46 \times 10^3\,\mathrm{J/(kg\,^{\circ}C)} \tag{7}$$

Q_{C_1}: aluminum solution heat, J; Q_{c_2}: reaction heat of oxygen and Al, J; W_{steel}: steel weight, kg; W_{Al}: Al weight, kg; [%O]: dissolved oxygen content, %; Q_c: total heat of reaction for Al, J; C_{P}: specific heat capacity of molten steel, J/kg °C.

After RH decarburization processing, Al particles are used in deoxidation. According to the condition of 105 t molten steel and 0.04% content of $[\mathrm{Al}]_{\mathrm{s}}$ in steel, the amount of Al added in RH refining process is shown in Fig. 7. For the original process, it has a large number and it fluctuates greatly. The aluminum added in the third heat is 201 kg, and the average Al added is 170 kg, which is

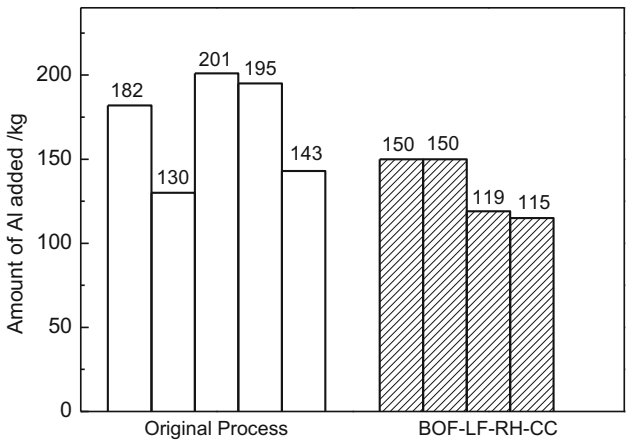

Fig. 7 Amount of aluminum added during RH refining process

significantly higher than average 133.5 kg in the BOF–LF–RH–CC process.

During RH decarbonization stage, the temperature rise through Al addition should not only be reasonable for the amount of aluminum addition, but also control the oxygen blowing timing and oxygen blowing intensity. If oxygen blowing is too early, it will not only damage the refractory material at the bottom of connecting pipe, but also delay the improvement in vacuum degree in the vacuum room, thus slowing the decarburization speeding. If oxygen blowing is too late, it will not be conducive for the timely release of CO gas, and the decarburization will be incomplete due to low dissolved oxygen content in molten steel. Through the BOF–LF–RH–CC process, RH furnace temperature is more stable, hence reducing the Al addition ratio in RH refining decarburization stage, which can not only reduce RH refining cost, but also improve RH refining effect.

3.3 T [O] and Sulfur Content Control in Molten Steel

3.3.1 T [O] Control in Molten Steel

The dissolved oxygen reflects the cleanliness of molten steel. Figure 8a shows variation of dissolved oxygen in the original process; Fig. 8b shows variation of dissolved oxygen in the BOF–LF–RH–CC process. As can be seen from Fig. 8, both two refining processes have same oxygen-level variation trend in the RH refining stage. In addition, by comparing variation of dissolved oxygen in RH refining process, it can be found that:

(1) Compared with the original process, the BOF–LF–RH–CC process reduces the RH inlet oxygen level. Except the 1st heat, where T [O] is 460×10^{-6}, the average of other three heats oxygen level is nearly 300×10^{-6}, while the original process average oxygen level is 450×10^{-6}.
Using the BOF–LF–RH–CC process can reduce inlet T [O] by about 150×10^{-6} compared with the original process. The reason is in BOF–LF–RH–CC process, high aluminum complex refining slag is added in LF refining process which reacts with dissolved oxygen in molten steel. High-aluminum complex refining slag can not only reduce the content of dissolved oxygen in molten steel, but also reduce the content of (FeO) and (MnO) in refining slag.

(2) Two different refining processes have same deoxidation rate which starts from RH decarburization stage for 5 min to the end of decarburization. During 10 min, the dissolved oxygen level drops by about 70×10^{-6}.After decarburization, the dissolved oxygen content of the original process is about 350×10^{-6}, on the contrary, it is about 275×10^{-6} for the BOF–LF–RH–CC process. The inlet oxygen

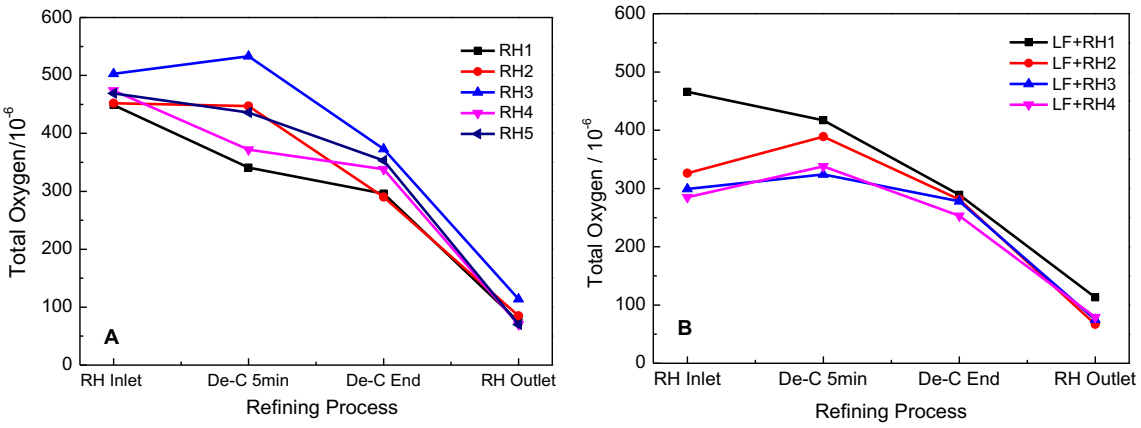

Fig. 8 Variation of dissolved oxygen in RH refining process

level of molten steel determines the T[O] at the end of decarbourization.

(3) After the end of decarburization, the vacuum degree is maintained at 1.5 mbar. By adding aluminum particles, two different refining way have same deoxidation rate, too. Within 15 min, the oxygen level decreases by about 250×10^{-6}.

(4) Finally, the original RH terminal total oxygen content is 80×10^{-6}, and that for the BOF–LF–RH–CC process is 70×10^{-6}. Therefore, the BOF–LF–RH–CC process can reduce the terminal T[O] content effectively.

3.3.2 Sulfur Content Control in Molten Steel

The average chemical compositions of steel during different refining processes are listed in Table 2.

Sulfur content changes in the refining processes are shown in Fig. 9.

In the original RH processing, the molten steel [S] % is 0.006%. By comparing the RH refining inlet steel compositions and refining terminal steel compositions in Fig. 9, it can be seen that the average [S] % in LF process is reduced from 0.0100 to 0.0030%.

The original refining process can effectively control the [S] % in steel by adding LF furnace [17]. It is because lime and high aluminum complex refining slag are added in LF refining process. By adding them, the content of dissolved oxygen in molten steel decreases rapidly. At the same time, reducing dissolved oxygen of steel is favorable for desulfurization.

LF deoxidation reactions are shown as follows:

$$2[\mathrm{Al}] + 3[\mathrm{O}] = \mathrm{Al_2O_3} \tag{8}$$

$$\mathrm{Al} + 3/2(\mathrm{FeO}) = 3/2\mathrm{Fe} + 1/2(\mathrm{Al_2O_3}) \tag{9}$$

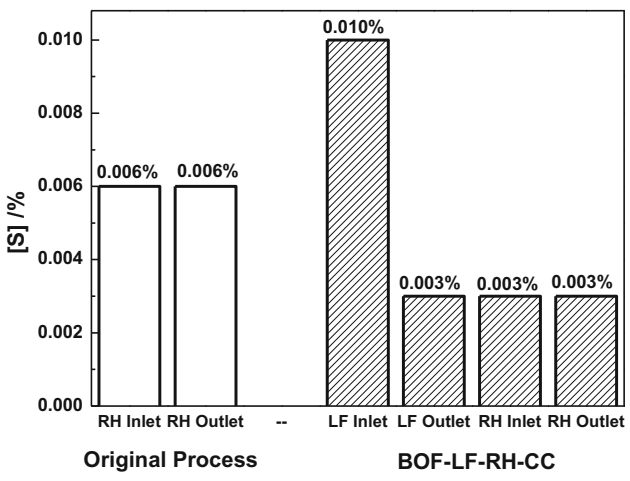

Fig. 9 Sulfur content in molten steel during refining process

Adding Al particle can improve CaO desulfurization effect. If Al particle is not added, silicate ($2CaO{\cdot}SiO_2$, $3CaO{\cdot}SiO_2$) is formed on the surface of lime, and the sulfur concentration is less than 5%.After the addition of aluminum, the lime surface generates $12CaO{\cdot}7Al_2O_3$, $2CaO{\cdot}FeO$, $4CaO{\cdot}Al_2O_3{\cdot}FeO$ and $2CaO{\cdot}SiO_2$, with sulfur content up to 10–0%, and the generated calcium aluminate has a greater capacity to dissolve sulfur [15, 16]. Adding aluminum to desulfurizer can accelerate desulfurization reaction of CaO.

With the participation of aluminum, the total reaction formula of CaO desulfurization is as follows:

$$2[\mathrm{Al}]+3[\mathrm{S}]+3(\mathrm{CaO}) = 3(\mathrm{CaS})+(\mathrm{Al_2O_3}) \tag{10}$$

$$\log_{10} k = \log_{10} \frac{a^3_{(\mathrm{CaS})} \cdot a_{(\mathrm{Al_2O_3})}}{a^3_{(\mathrm{CaO})}} \cdot \frac{1}{a^2_{[\mathrm{Al}]} \cdot a^3_{[\mathrm{S}]}} \tag{11}$$

$$\Delta G = -31487 - 67.53T \tag{12}$$

The CaS and calc-aluminate activity are calculated by FactSage, and the CaS activity is 0.91 at 1600 °C. The activity of calcium aluminate is shown in Table 3. By putting the activity value into Eq. (11) to calculate, and the equilibrium curve of [Al]–[S] under different equilibrium states at 1600 °C is shown in Fig. 10.

Table 3 Different calcium aluminate activity coefficients in 1600 °C

Calcium aluminate	Al_2O_3 activity	CaO activity
$CaO{\cdot}6Al_2O_3$	1.000	0.005
$CaO{\cdot}2Al_2O_3$	0.287	0.103
$CaO{\cdot}Al_2O_3$	0.180	0.166
$12CaO{\cdot}7Al_2O_3$	0.050	0.433
$3CaO{\cdot}Al_2O_3$	0.009	0.992

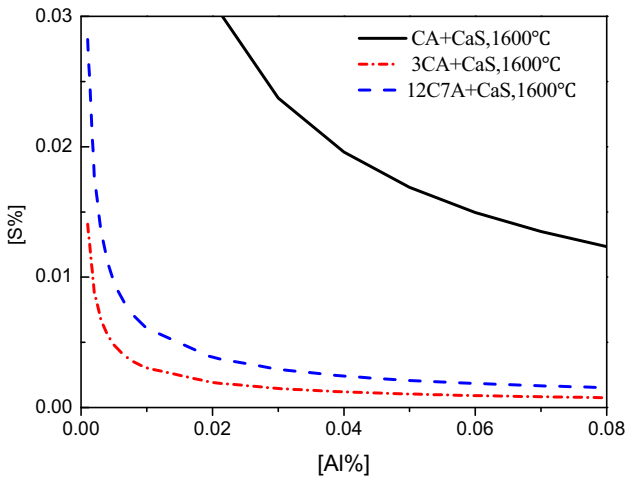

Fig. 10 [Al]–[S] equilibrium curves under different equilibrium states

When $[Al]_s$ in steel is constant, with the increase of [Ca], the sequence of calcium aluminate generated is: $CaO{\cdot}Al_2O_3 \rightarrow 12CaO{\cdot}7Al_2O_3 \rightarrow 3CaO{\cdot}Al_2O_3$ [18]. According to Fig. 10, when $[Al]_s$ in steel is a constant value, [S] in liquid steel decreases significantly as [Ca] increases. When [Ca] in steel is constant, [S] in liquid steel gradually decreases with increasing $[Al]_s$. In LF refining process, the addition of appropriate lime and high aluminum complex refining slag can significantly reduce the sulfur content in the molten steel from 0.0100 to 0.0030%. The BOF–LF–RH–CC process can control the sulfur content of molten steel effectively.

3.4 Inclusion Control Situation

3.4.1 Change of Inclusion Quantity and Size

Figure 11a shows the comparison of inclusion area per square millimeter steel sample at the RH refining-end under different refining processes.

In Fig. 11a, inclusion control level fluctuates greatly in the original refining process, the 2nd heat has the best inclusion control level with inclusion area of 189 $\mu m^2/mm^2$; the 3rd heat had the worst inclusion control level with inclusion area of 404 $\mu m^2/mm^2$; the reasons for the unsatisfactory inclusions control level in the 3rd heat are due to 505×10^{-6} RH inlet oxygen level and the amount of aluminum added in the whole refining process is 201 kg. Compared with the 2nd heat RH inlet oxygen level of 452×10^{-6}, adding 130 kg of aluminum in the whole refining process and under the condition that the finished product control $[Al]_s$ is 0.04% and the circulation time is 6 min, the 3rd heat generates more Al_2O_3 inclusions. The 1st heat RH inlet oxygen level is 453×10^{-6} on adding 182 kg of aluminum in the whole refining process; the 4th heat RH inlet oxygen level is 470×10^{-6} on adding 195 kg of aluminum in the whole refining process; the 5th heat RH inlet oxygen level is 469×10^{-6} on adding 143 kg of aluminum in the whole refining process.

The RH inlet oxygen level of the 1st heat is almost the same as that of the 2nd heat; however, the amount of aluminum added in the 1st heat is 50 kg more than that in the 2nd heat. This is because inlet molten steel temperature of the 1st furnace is 1636 °C, the 2nd is 1652 °C. Except deoxidation and alloying, aluminum added in the 1st heat also heat molten steel temperature during the decarburetization stage. This situation also exists in the 4th and 5th heat comparison of the original refining process.

The RH inlet temperature of the 2nd and 5th heat is higher than 1650 °C, so both two heats do not need to add Al to heat up molten steel temperature during the decarburetization stage. The oxygen level 452×10^{-6} in the 2nd heat is lower than that in the 5th furnace 469×10^{-6}; as a consequence, the aluminum addition in the 2nd heat is less than that in the 5th heat, and the inclusion area in the 2nd heat is less than that in the 5th heat.

Using the BOF–LF–RH–CC process, the 3rd heat has the best inclusion control level with inclusion area of 202 $\mu m^2/mm^2$; the 2nd heat has the worst inclusion control level with inclusion area of 278 $\mu m^2/mm^2$. The 3rd heat RH inlet oxygen level is 285×10^{-6} on adding 115 kg of aluminum in the whole refining process; the 2nd heat RH inlet oxygen level is 285×10^{-6} on adding 150 kg of aluminum in the whole refining process.

Figure 11b shows the single inclusion area comparison between the original process and the BOF–LF–RH–CC process. The critical area of steel surface inclusion affecting fatigue performance is 8 μm^2, and when the area of a single inclusion is less than 8 μm^2, it is considered that it has no effect on steel quality [16, 19]. Compared with the original process, single inclusion area of < 8 μm^2 proportion increases from 85 to 95% for the BOF–LF–RH–CC process.

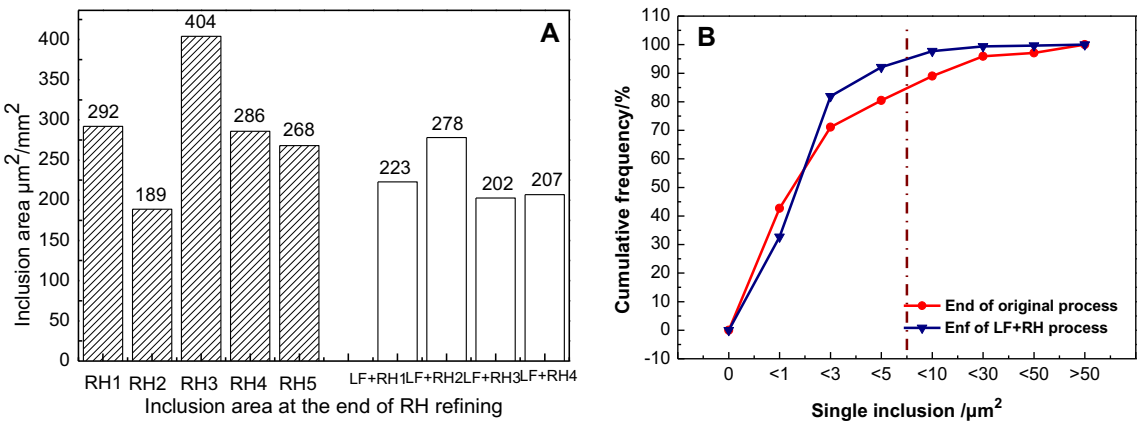

Fig. 11 Inclusion area comparison at the end of RH refining

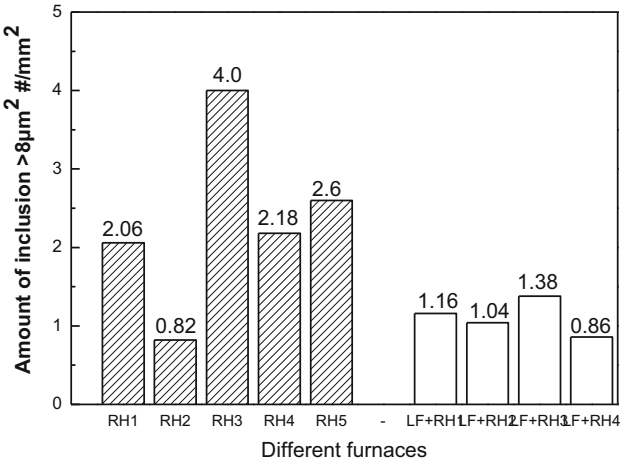

Fig. 12 Inclusion amount at the end of RH refining #/mm^2

Figure 12 shows the inclusion amount of RH refining-end steel samples. The control of inclusion amount in the original process does not remain steady. The inclusion amount of the 2nd heat is 0.82/mm^2, the inclusion amount of the 3rd heat is 4.0/mm^2, and the average inclusion amount of inclusions is 2.33/mm^2. In the BOF–LF–RH–CC process, inclusion amount of the 3rd heat is 1.38/mm^2, the inclusion amount of the 4th heat is 0.86/mm^2, and the average inclusion amount of inclusions is 1.11/mm^2.

Compared with the original process, the BOF–LF–RH–CC process can lower RH inlet dissolved oxygen level, reduce the amount of aluminum particles added, stabilize the control level of inclusions and significantly improve the cleanliness of liquid steel.

For the reason that Al deoxidation has been used in this steel, the evolution of Al_2O_3 inclusion size under different refining processes has further been studied. The size distribution of Al_2O_3 inclusions in two processes is shown in Fig. 13. Figure 13a, b shows the area distribution of Al_2O_3 inclusions after RH breaking through the original process and BOF–LF–RH–CC process, respectively. According to Fig. 13a, the inclusion area of Al_2O_3 in all original process furnaces is evenly distributed, and the Al_2O_3 inclusions less than 10 μm^2 in molten steel is about 70%, and that of Al_2O_3 inclusions less than 5 μm^2 in molten steel is about 50%; According to Fig. 13b which presents the inclusion area of Al_2O_3 in the BOF–LF–RH–CC process, the proportion of Al_2O_3 inclusions less than 10 μm^2 in molten steel is about 85%, and that of Al_2O_3 less than 5 μm^2 in molten steel is about 70%. In the BOF–LF–RH–CC process, the proportion of small-sized inclusions is higher than that of the original process.

3.4.2 *Reasons for Improving the Cleanliness of the BOF–LF–RH–CC Process*

The reason that the BOF–LF–RH–CC process can significantly improve the cleanliness of liquid steel can be attributed to:(1) LF furnace can heat molten steel, so it can avoid heating up of Al added during the decarburization of RH operation, (2) LF furnace can blow argon for stirring to promote inclusion rise and better control of the cleanliness of liquid steel.

In the ladle argon blowing refining process, liquid steel is in a turbulent state, the rate of inclusion floating and removal consists of two aspects. One is the floating rate of the inclusion itself based on Stokes equation, and the other is the floating rate of the inclusion captured by argon bubbles.

Under laminar flow conditions, the floating velocity of inclusions can be calculated by Stokes Eq. (13):

$$u_s = \frac{g(\rho_{\text{steel}} - \rho_{\text{inclusion}})d^2_{\text{inclusion}}}{18\mu_{\text{steel}}} \tag{13}$$

In Eq. (13), g represents the acceleration of gravity, g = 9.8 m/s^2; ρ_{steel}, $\rho_{\text{inclusion}}$ is density of molten steel and

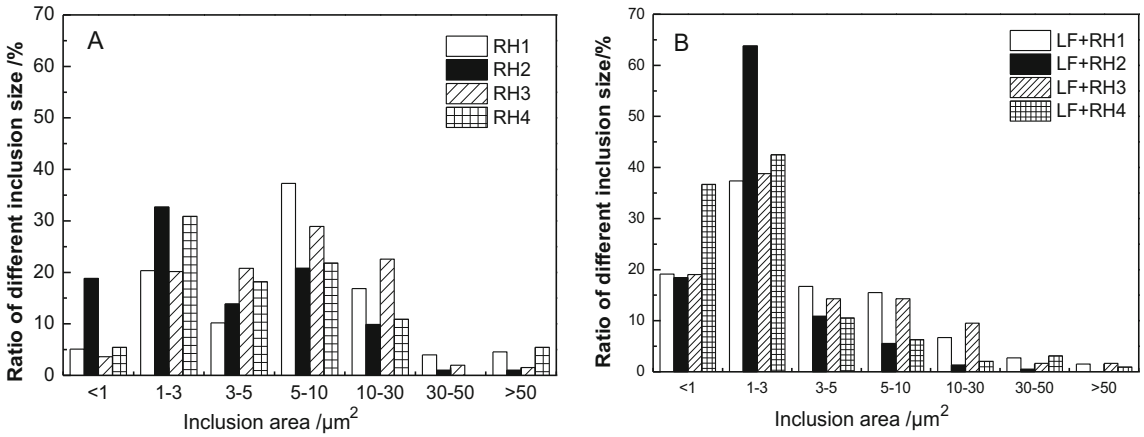

Fig. 13 Al_2O_3 inclusion distribution in different refining processes

inclusions, kg/m^3; μ_{steel} is kinematic viscosity of liquid steel, Pa s; $d_{inclusion}$ is inclusion diameter, m.

According to Eq. (13), the floating speed of the inclusion Stokes is related to the diameter of the inclusion. With the increase in inclusion's diameter, the Stokes floating speed increases.

Zhang and Taniguchi [20] discussed the influence of bubble flotation on inclusion removal rate of different sizes by establishing a simplified model, but he ignored the influence of turbulence on inclusion removal by bubble flotation. The calculated removal rate of large-sized inclusion is higher than small-sized inclusion. It also explains that turbulence must be considered for the inclusion bubble flotation removal in LF refining process. Duan et al. [21] considered the influence of turbulence on bubble flotation to remove inclusions. He found that in the Ar bubble column, the liquid steel of the turbulent kinetic energy is at around 10^{-1}m^2/s^2, while utilizing the bubble flotation to remove inclusions that are mainly concentrated in the Ar bubble column. Under the condition of the turbulent kinetic energy, the catching probability of a single bubble for inclusions of different sizes is basically the same.

Based on the limited data available, the turbulence condition inclusion removal formula is as follows:

$$\frac{dn_{inclusion}}{dt} = -\frac{2u_0}{H} \cdot \frac{\alpha_P}{100} \cdot n_{inclusion} \quad (14)$$

$$\alpha_P = 2.39 + 573.12 \cdot Q \quad (15)$$

$$u_0 = 0.22 + 3.48 \cdot Q - 158.08 \cdot Q^2 \quad (16)$$

In equation, u_0 is the average rising velocity of molten steel in the plume region, m/s; α_P represents the volume fraction of the plume area of the ladle blowing argon column, %; $n_{inclusion}$ is the total number of inclusions in the furnace; Q is Argon flow rate of ladle blowing, m^3/s.

The current LF furnace argon flow rate is 220 NL/min, under the condition that the inclusion diameter is 1 μm; 10 μm;100 μm, Stokes floating speed and inclusion flotation speed are calculated, respectively. Figure 14 shows the change of inclusion removal rate with time with the inclusion diameters of 1 μm; 10 μm; 100 μm.

According to Fig. 14a, b, when the inclusion diameters are 1 μm and 10 μm, the inclusion size is small and Stokes floating speed is slow. Compared with Stokes floating removal, bubble flotation is the main inclusion removal method. Under the condition of argon blowing and stirring, almost all 1 μm inclusions are removed by bubble flotation. The ratio of 10 μm inclusion's removal by bubble flotation is about 3 times than Stokes floating removal. It can be seen that ladle argon blowing and stirring can significantly increase the proportion of inclusion removal.

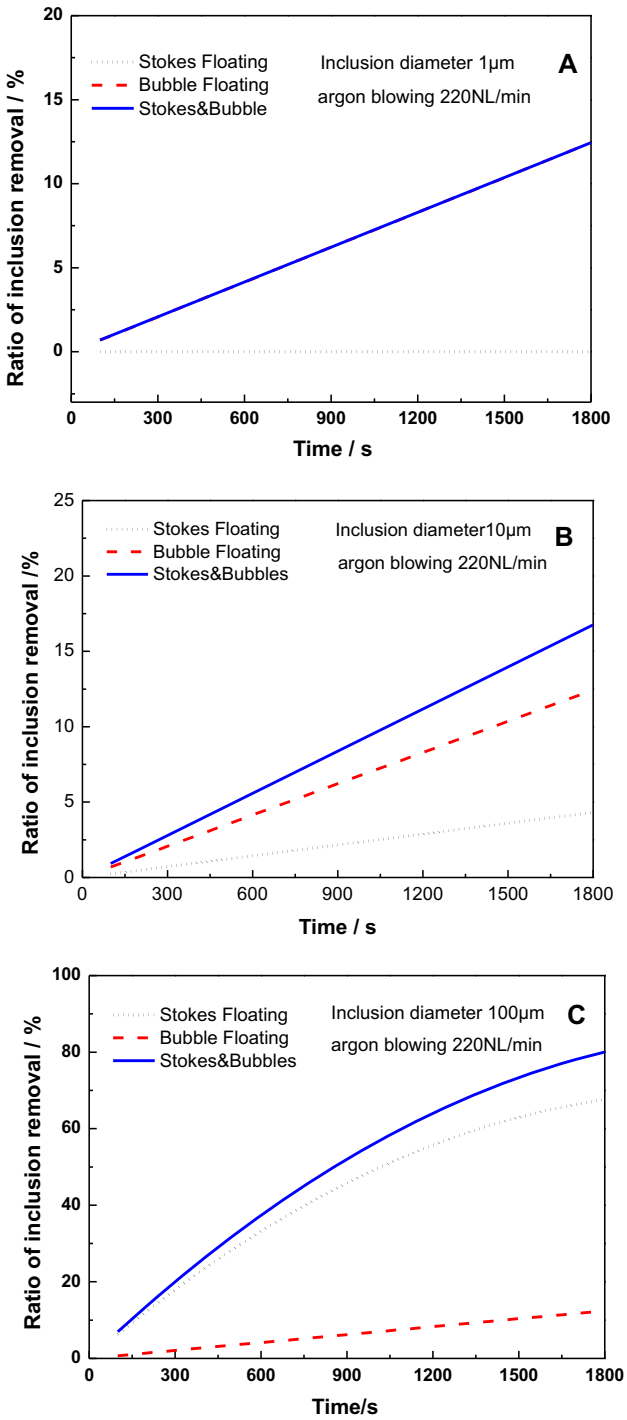

Fig. 14 Inclusion removal fraction as a function of time for different removal conditions with inclusion diameter of 1 μm, 10 μm, 100 μm

It can be seen from Fig. 14c, when inclusion diameter is 100 μm, Stokes' floating speed cannot be ignored due to large size of inclusion, and Stokes' floating has become the main way to remove inclusion.

In order to further compare the LF refining process in the removal effect of different dimension of inclusions, this

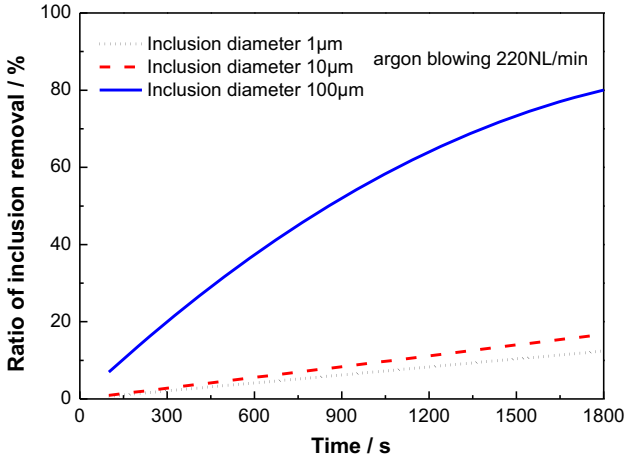

Fig. 15 Inclusion removal rate for different inclusion diameters

paper has calculated inclusion removal rate with time for which the inclusion diameters are 1 μm, 10 μm, 100 μm. In this calculation, LF furnace argon gas flow is 220 NL/min and both bubble flotation and Stokes floatation have been considered. Figure 15 shows inclusion removal rate for different inclusion diameters.

According to Figs. 14 and 15, when the size of inclusions are 1 μm and 10 μm, the floating speed of Stokes is relatively small compared with Ar flow field. The main way to remove inclusions is bubble flotation. Nevertheless, when the inclusion size is 100 μm, the floating speed of Stokes can't be ignored; moreover, Stokes floating removal will be the main way to remove inclusions.

Recently, in the BOF–LF–RH–CC process, the LF refining time is about 35 min. Molten steel temperature increases effectively throughout the period. LF refining also has functions of controlling the composition of molten steel and reducing non-metallic inclusions. Argon blowing and stirring in LF furnace can significantly reduce the amount of inclusions. For 10 μm-diameter sized non-metallic inclusions, the removal rate of LF refining process can be close to 15%; moreover, for 100 μm-diameter large-sized non-metallic inclusions, the removal rate of LF refining process can become more than 80%.

Al_2O_3 inclusion has the characteristics of high melting point, poor wettability with steel liquid and easy to rise to slag for removal. Strong circulating stirring of molten steel under RH refining vacuum condition promotes Al_2O_3 inclusion's collision polymerization in molten steel, at the same time, the floating removal of Al_2O_3 inclusions is promoted by molten steel circulation; which reduces the quantity and density of inclusions. After adopting the BOF–LF–RH–CC process, the amount of Al added in RH stage is reduced; the proportion of large-sized Al_2O_3 inclusions in molten steel is reduced, too. For the BOF–LF–RH–CC process, it has less addition of Al in decarbonization stage and less deoxidation products compared with the original process, so it produces less Al_2O_3 inclusions. In the limited refining time, the BOF–LF–RH–CC process' Al_2O_3 inclusions removal efficiency is obviously higher than that of the original process. After RH refining, Al_2O_3 inclusions in the BOF–LF–RH–CC process are smaller in size and less in quantity than original process.

4 Conclusions

In view of the problem that the RH temperature fluctuates greatly in the production of ultra-low carbon Al-killed steel by BOF–RH–CC, and Al addition heat up of RH process decreases the cleanliness degree of molten steel, this study puts forward the new production process of BOF–LF–RH–CC and compares the evolution of temperature, aluminum content, sulfur content, oxygen content and inclusions in the two processes. The main conclusions are as follows:

(1) In the converter—RH—continuous casting process, RH inlet temperature fluctuates greatly, the lowest temperature is 1621 °C; the highest temperature is 1662 °C. Unstable RH inlet temperature is not conducive to industrial operation; after adopting the new refining process, RH inlet temperature is stable to around 1650 °C.

(2) The sulfur content of RH outbound steel liquor in the new refining process is significantly reduced, from 0.0100 to 0.0030% on average, while the sulfur content of RH outbound is 0.006% in the original process.

(3) Both refining processes can decrease the total oxygen content of steel. BOF–LF–RH–CC process has lower oxygen content at the endpoint of refining than original process. The average aluminum addition in the original process is 175 kg, and the total oxygen content after RH refining is 0.0080%. The RH incoming oxygen content in the BOF–LF–RH–CC process is significantly reduced, with the average aluminum addition in the process being 133.5 kg, and the total oxygen mass fraction after RH refining is 0.0070%.

(4) Two processes can reduce the inclusion area fraction and quantity density in the steel adequately. After adopting BOF–LF–RH–CC process refining, the average inclusion area fraction after RH treatment decreases from 289.8 to 227.5 $\mu m^2/mm^2$, at the same time proportion of inclusion size less than 8 μm^2 increases from 85 to 95% compared with original process. The proportion of Al_2O_3 inclusions less than 5 μm^2 increases from about 50% to more than 70%.

The proportion of inclusions bigger than 5 μm^2 is significantly reduced after the new refining process. The new refining process is more beneficial to control the size of Al_2O_3 inclusions and reduce the impact of inclusions on the cleanliness of liquid steel.

(5) The new refining process has more advantages than the original process in the aspects of temperature stability of molten steel, control of impurity elements and inclusions and is more suitable for the production of ultra-low carbon Al-killed steel with higher cleanliness requirements.

Acknowledgement This work was financially supported by National Key R&D Program of China (2017YFB0304000).

References

1. Guo J, Bao Y, and Wang M, *Int J Miner Metall Mater* **24** (2017) 1370.
2. Deng X, Li L, Wang X, Ji Y, Ji C, and Zhu G, *Int J Miner Metall Mater* **21** (2014) 531.
3. Xiao C, and Cui H, *Chin J Eng* **S1** (2018) 26.
4. Hu Y, Chen W, Wan C, Wang F, and Han H, *Metall Mater Trans B* **49** (2018) 569.
5. Ma H, Wang X, Huang F, Ji C-X, and Pan H-W, *Iron and Steel* **51** (2016) 19 **(in Chinese)**.
6. Yang W, Wang X, Zhang L, Shan Q, and Liu X, *Steel Res Int* **84** (2013) 473.
7. Shu H, Liu L, Liu X, and Zhang XF, *J Iron Steel Res* **18** (2011) S2.
8. Qin Y, Wang X, Huang F, Chen B, and Ji C, *Metall Res Technol* **112** (2015) 405.
9. Park D-C, Jung I-H, Rhee P C H, and Lee H G, *ISIJ Int* **44** (2004) 1669.
10. Wang C, Verma N, Kwon Y, Tiekink W, Kikuchi N, and Sridhar S, *ISIJ Int* **51** (2011) 375.
11. Rout B K, Brooks G, Rhamdhani M A, Li Z, Schrama F N, and Sun J, *Metall Mater Trans B* **49** (2018) 537.
12. Li C W, Cheng G G, Wang X H, Zhu G S, and Cui A M, *Iron Steel* **47** (2012) 7.
13. Li P, Bao Y, Yue F, Peng Z, and Yuan X F, *Chin J Eng* **33** (2011) 823 **(in Chinese)**.
14. Li C, Cheng G, Wang X, Zhu G S, and Cui A M, *Steelmaking* **27** (2011) 35 **(in Chinese)**.
15. Cui H, Tian E, and Chen B, *Chin J Eng*, **35** (2014) 32 **(in Chinese)**.
16. Wang Y, Bao Y, Heng C U, Bin C H, and Ji C X, *J Iron Steel Res Int* **19** (2012) 1.
17. Wu L, Pei F, Chen Y, and Li S Q, *J Iron Steel Res Int* **19** (2012) 17.
18. Fang Z, *Study on the Control of Inclusion in the 27CrMoV Oil Casing Steel*, University of Science and Technology Beijing (2016).
19. Wang H, *Investigation of Inclusion Control and Evolution During Electroslag Remelting for H13 Steel*, University of Science and Technology Beijing.
20. Zhang L, and Taniguchi S, *Metall Rev* **45** (2014) 59.
21. Duan H, Ren Y, and Zhang L, *Steel Res Int* **90** (2019) 1.